CRYSTAL GROWTH & DESIGN

Article

pubs.acs.org/crystal

Ortho-Substituent Effects on Diphenylurea Packing Motifs

Marina A. Solomos, Taylor A. Watts, and Jennifer A. Swift*

Department of Chemistry, Georgetown University, 37th and O Streets NW, Washington, DC 20057-1227, United States

Supporting Information

ABSTRACT: Hydrogen bonding between urea groups is a widely used motif in crystal engineering and supramolecular chemistry studies. In an effort to discern how the steric and electronic properties of substituents affect the molecular conformation and crystal packing of ortho-substituted *N*,*N*′-diphenylureas (*o*PUs), herein we report the synthesis, characterization, and polymorph screening of eight members of this family. Of the 16 total *o*PU structures known (including nine structures from this study and seven previously reported), only two are isostructural. These 16 structures are sorted into three general architecture types based on their hydrogen bond topologies. In Type I, urea molecules related by translation form linear one-dimensional (1D) hydrogen bonded chains. In Type II, urea molecules rotate about a 1D hydrogen bond axis forming twisted chains. Urea groups do not hydrogen bond to one another in Type III. Energy calculations performed at the B3LYP/6-31G(d,p) level show a higher rotational barrier about the amide bond in *o*PUs compared to meta-substituted diphenylureas (*m*PUs), which may explain the smaller range of torsion angles observed in *o*PUs compared to *m*PUs. Although ortho-substitution does not seem to limit the hydrogen bonding between urea groups in most cases, a notably higher percentage of *o*PU phases are polar compared to PUs with other substitution patterns. This suggests restricted conformations might offer some advantage in achieving acentric materials.

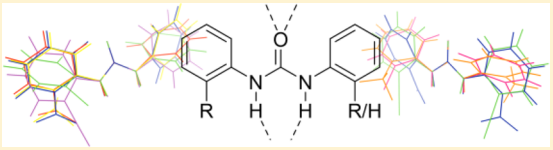

INTRODUCTION

N,*N*′-Phenylurea (PU) is an interesting core unit that appears in a wide range of chemical compounds with diverse applications. It is found in pharmaceuticals developed to treat diseases ranging from African sleeping sickness[1] to psoriasis[2] and cancer.[3,4] PUs have also attracted negative attention for their persistence in the environment due to their use as herbicides[5−7] and as antibacterial ingredients in personal care products (e.g., triclocarban).[8−10] The persistence of hydrogen bonding between urea groups has also enabled the assembly of urea-based supramolecular materials such as gels, tubes, and capsules.[11−13] In the crystalline state, PUs have served as model systems for crystal polymorphism studies[14−19] and been explored as possible nonlinear optical materials.[20−23]

To better exploit the properties of PUs in these various applications, some of our recent efforts have focused on defining under what conditions the urea hydrogen bonding motif ceases to be reliable. This idea was first probed by Etter in the late 1980s in studies which showed that some diphenylureas with electron withdrawing substituents cocrystallized with other strong hydrogen bond donor and acceptor molecules.[16,24,25] More recently, we showed that the ability to disrupt urea hydrogen bonding in a series of meta-substituted diphenylureas (*m*PUs) with the strong hydrogen bond acceptor triphenylphosphine oxide (TPPO) can be reasonably well predicted based on differences in the relative energies of urea···urea and urea···TPPO dimers.[26]

In the current study, we attempt to address the question of how steric effects play a role in the urea assembly motifs. A search of the Cambridge Structure Database V5.38 (November 2016) for low molecular weight PUs with only ortho-substituents yielded just seven structures. In an effort to expand our structure analysis set, we prepared eight *o*PUs, screened them for polymorphism, and determined nine new single crystal structures. Analysis of all new and previously reported crystal structures revealed 15 unique packing arrangements and only one isostructural pair. Calculations validate our assumption that ortho-substituents present a significant steric barrier to rotation about the amide bond and hydrogen bonding between urea groups.

EXPERIMENTAL SECTION

Materials. All 2-X-isocyanate and 2-Y-aniline reagents were obtained from Sigma-Aldrich (97−99%) or Combi-Blocks and used without further purification. All solvents used in synthesis and crystallization experiments were reagent grade or higher and were obtained from Sigma-Aldrich, Fischer Scientific, and Warner-Graham. ^{1}H NMR data were collected on a 300 MHz Varian Inova Spectrometer in d_6-DMSO.

Synthesis. Symmetrical and unsymmetrical ortho-substituted diphenylureas were synthesized according to previously reported methods.[25] For each compound, equimolar amounts of 2-X-isocyanate and 2-Y-aniline were dissolved in benzene or dichloromethane flushed with nitrogen and stirred at RT for 24 h. Gentle heating was often required for full dissolution. After 24 h, the product was isolated using vacuum filtration and recrystallized in ethanol or acetonitrile. Product synthesis was confirmed by ^{1}H NMR and melting point. Single crystals used in structure determination were grown from ethanol except where otherwise indicated.

1,3-Bis(o-trifluoromethylphenyl)urea (oCF$_3$PU). Prepared from 2-trifluoromethylaniline and 2-(trifluoromethyl)phenylisocyanate. Recrystallization in ethanol yielded colorless needles with mp = 230.0−

Received: May 31, 2017
Revised: August 8, 2017

DOI: 10.1021/acs.cgd.7b00757
Cryst. Growth Des. XXXX, XXX, XXX−XXX

Table 1. Crystallographic Data for Diphenylureas with Ortho-Substituents (N = Nitro, Cl = Chloro, CF_3 = Trifluoromethyl, Cy = Cyano)

urea	β-oNPU	α-oNHPU	β-oNHPU	oClPU	oClHPU	oCF$_3$PU	oCF$_3$HPU	oCyPU	oCyHPU
formula	$C_{13}H_{10}N_4O_5$	$C_{13}H_{11}N_3O_3$	$C_{13}H_{11}N_3O_3$	$C_{13}H_{10}Cl_2N_2O$	$C_{13}H_{11}ClN_2O$	$C_{15}H_{10}F_6N_2O$	$C_{14}H_{11}F_3N_2O$	$C_{15}H_{10}N_4O$	$C_{14}H_{11}N_3O$
temp (K)	110	100	173	110	110	100	100	296	100
space group	$P\bar{1}$	Pc	$P2_1/c$	$P2/n$	$Pna2_1$	$P2_1/n$	$Pna2_1$	$P2_1/n$	$P2_1/c$
a (Å)	9.9134(12)	4.6327(3)	4.62450(10)	15.9459(10)	9.1866(7)	4.6101(2)	13.9832(11)	7.4598(4)	5.44700(10)
b (Å)	11.5929(12)	6.1305(4)	20.3783(8)	4.6128(2)	11.1288(9)	13.8352(6)	19.2797(14)	12.4052(7)	19.9264(5)
c (Å)	12.7294(13)	20.9967(15)	12.631	16.3242(9)	11.4667(9)	22.3435(10)	4.6241(4)	13.2127(8)	10.8499(2)
α (deg)	109.635(9)	90	90	90	90	90	90	90	90
β (deg)	111.993(10)	92.603(2)	99.020(4)	90.520(5)	90	94.125(3)	90	100.923(4)	103.3450(10)
γ (deg)	91.207(9)	90	90	90	90	90	90	90	90
V (Å^3)	1259.4(3)	595.707	1175.62	1200.68	1172.31	1421.41	1246.62	1200.56	1145.84
Z	4	2	4	4	4	4	4	4	4
R	0.0504	0.0238	0.0426	0.0480	0.0404	0.0432	0.0572	0.0428	0.035
R_w	0.1166	0.0605	0.1148	0.1516	0.0970	0.1195	0.1354	0.1304	0.0846
type	III	I	I	I	II	I	I	III	III
crystal habit	prism	needle	needle	needle	needle	needle	needle	prism	prism

232.0 °C. ^{1}H NMR (DMSO-d_6, ppm) δ: 7.90, (s, 2H); 7.00, (d, 2H); 6.85, (m, 4H); 6.51, (t, 2H).

1-(o-Trifluorophenyl)-3-phenylurea (oCF$_3$HPU). Prepared from phenylisocyanate and 2-trifluoromethylaniline. Recrystallization in ethanol yielded colorless needles with mp = 175.5−178.8 °C. ^{1}H NMR (DMSO-d_6) δ: 8.55, (s, 1H); 7.25, (s, 1H); 7.12, (d, 1H); 6.83, (m, 2H); 6.64, (d, 2H); 6.48, (m, 3H); 6.17, (t, 1H).

β-1,3-Bis(o-nitrophenyl)urea (β-oNPU). Prepared from 2-nitrophenylisocyanate and 2-nitroaniline. Recrystallization in ethanol yielded colorless crystals with mp = 210.2−215.9 °C (lit. 225−227 °C[27]). ^{1}H NMR (DMSO-d_6, ppm) δ: 9.21, (s, 2H); 7.20, (dd, 2H); 7.12, (dd, 2H); 6.87, (m, 2H); 6.46, (m, 2H). The β-oNPU structure was determined from a plate grown from benzene.

1-(o-Nitrophenyl)-3-phenylurea (oNHPU). Prepared from phenylisocyanate and 2-nitroaniline. Recrystallization in ethanol yielded colorless needles (β-oNHPU) with mp = 163.0−166.6 °C (lit. 170 °C[28]). ^{1}H NMR (DMSO-d_6) δ: 9.82, (s, 1H); 9.58, (s, 1H); 8.29, (dd, 1H); 8.09, (m, 1H); 7.70, (m, 1H); 7.49, (m, 2H); 7.31, (m, 2H); 7.21, (m, 1H); 7.02, (m, 1H). Recrystallization in acetone yielded yellow needles (α-oNHPU) with a mp = 171.0−173.4 °C.

1,3-Bis(o-chlorophenyl)urea (oClPU). Prepared from 2-chloroaniline and 2-chlorophenylisocyanate. Recrystallization in ethanol yielded colorless needles with mp = 240.0−241.7 °C (lit. 240.5−241.5 °C[29]). ^{1}H NMR (DMSO-d_6, ppm) δ: 9.02, (s, 2H); 8.07, (dd, 2H); 7.47, (dd, 2H); 7.30, (dd, 2H); 7.06, (dd, 2H).

1-(o-Chlorophenyl)-3-phenylurea (oClHPU). Prepared from 2-chlorophenylisocyanate and aniline. Recrystallization in ethanol yielded thin white needles with mp = 185.1−188.4 °C (lit. 180−182 °C[30]). ^{1}H NMR (DMSO-d_6) δ: 9.41, (s, 1H); 8.31, (s, 1H); 8.17, (dd, 1H); 7.47, (m, 3H); 7.31, (m, 3H); 7.02, (m, 2H).

1,3-Bis(o-cyanophenyl)urea (oCyPU). Prepared from 2-aminobenzonitrile and 2-cyanophenylisocyanate. The reaction flask was left undisturbed after a 96 h stirring period such that crystals suitable for single crystal X-ray diffraction of the product could be obtained directly from the reaction mixture. The colorless prisms obtained undergo a phase change between mp = 154.9−178.8° and decompose with continued heating (lit. 250 °C (decomp)[31]). ^{1}H NMR (DMSO-d_6, ppm) δ: 9.44, (s, 2H); 8.03, (dd, 2H); 7.80, (dd, 2H); 7.63, (dd, 2H); 7.25, (dd, 2H).

1-(o-Cyanophenyl)-3-phenylurea (oCyHPU). Prepared from phenylisocyanate and 2-aminobenzonitrile. Recrystallization in ethanol yielded colorless prisms with a mp = 166.2−170.8 °C (lit. 163 °C (decomp)[31]). ^{1}H NMR (DMSO-d_6) δ: 8.57, (s, 1H); 7.92, (s, 1H); 7.27, (d, 1H); 6.93, (dd, 1H); 6.83, (m, 1H); 6.65, (m, 2H); 6.49, (m, 2H); 6.36, (m, 1H); 6.19 (m, 1H).

Crystal Growth and Polymorph Characterization. Crystallization by slow evaporation was attempted from a number of different solvents, including but not limited to acetone, toluene, acetonitrile, ethanol, methanol, benzene, 2-propanol, ethyl acetate, 1:1 hexanes/acetone, 1:1 hexanes/ethyl acetate, and chloroform. Vials with oPU and solvent were heated for complete dissolution, then covered with pierced Parafilm and maintained at room temperature for 2−10 days until crystallization was evident.

Optical and hot-stage microscopy (HSM), differential scanning calorimetry (DSC), and powder X-ray diffraction (PXRD) were used to characterize the solid state materials. Phase transitions in bulk and single crystal samples were identified by HSM using a HCS302 optical hot-stage with a standard deviation of ±1° up to 250° (INSTEC, Inc., Boulder, CO) interfaced with an Olympus BX-50 microscope. Melting points were determined by DSC using a TA Instruments Modulated DSC 2920. Samples were prepared in hermetically sealed aluminum pans using 2−10 mg of crystalline sample. All runs were performed at a heating rate of 5−10 °C/min. DSC data were analyzed with Universal Analysis software. PXRD data was collected on bulk ground samples at room temperature (5−40° in 2θ) on a Rigaku Ultima IV X-ray diffractometer (Cu Kα radiation, 40 kV tube voltage, 44 mA current). PXRD spectra were analyzed using Jade v9.0 software and compared against simulated PXRD patterns of known single crystal structures.

Single Crystal X-ray Structure Determination. Crystal structure determination was accomplished using a Siemans/Bruker SMART or APEX II Platform CCD diffractometer (Mo Kα radiation = 0.71073 Å) at 100 or 110 K in most cases. Intensity data was corrected for absorption and decay in SADABS.[32] Structures were solved in SHELXS and refined using SHELXL.[33] Non-hydrogen atoms were solved using direct methods and refined with anisotropic displacement parameters. Hydrogen treatment was mixed. Urea hydrogen atom positions were typically determined from the residual electron density, while most aromatic hydrogen atoms were placed in ideal positions and refined with a riding model. Cif files for all nine structures have been deposited in the CCDC 1504100−1504106 and 1504132−1504133.

Computational Methods. The rotational barrier about the amide bond in oClPU and oClHPU were calculated using *ab initio* molecular orbital calculations. Similar rotational barrier calculations for 1,3-bis(*m*-chlorophenyl)urea (mClPU) were also performed to directly compare ortho- and meta-substituent effects. Geometries at fixed torsion angles were optimized in Gaussian09 with ModRedundant constraints at the B3LYP/6-31G(d,p) level. *Anti* and *syn* refer to the orientation of the substituent relative to the carbonyl group (*syn* = −180°; *anti* = 180°). The planar *anti*−*syn* conformation was rotated in increments of 10 degrees toward the *anti*−*anti* conformation. Specifically, the phenyl ring bearing the *syn* substituent was rotated around the C(O)−N−C−C torsion angle between the carbonyl carbon and the aromatic carbon bound to the ortho-substituent. In the case of mClPU, the aromatic carbon closest to the meta-substituent

DOI: 10.1021/acs.cgd.7b00757
Cryst. Growth Des. XXXX, XXX, XXX−XXX

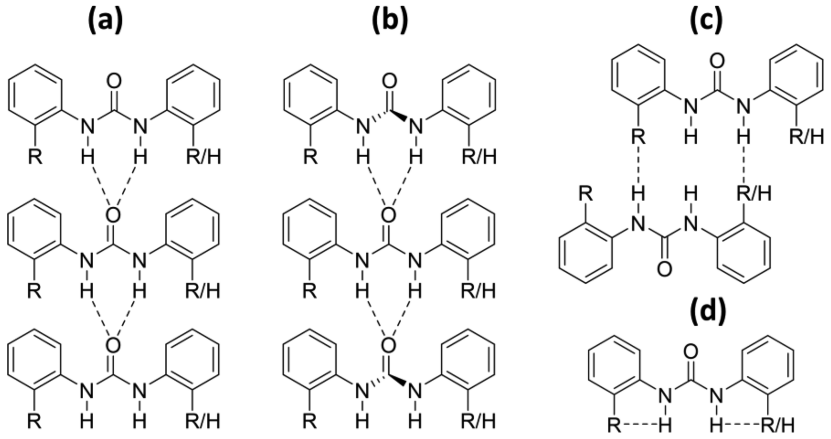

Figure 1. Different types of hydrogen bonding identified in *o*PUs: (a) Type I, (b) Type II, and (c,d) Type III.

Table 2. Torsion Angles and Hydrogen Bond Distances in *o*PUs

	urea chain axis	C(O)−N−C−C torsion angle (ortho substituent) (deg)	O···H−N distance (O···N distance) (Å)
*o*AHPU	*b* (Type I)	92.87 (A), −47.96 (H)	2.126 (2.932), 1.942 (2.771)
*o*BrPU	*c* (Type I)	−138.40 (Br), −138.40 (Br)	2.104 (2.917), 2.104 (2.917)
oCF_3PU	*a* (Type I)	116.52 (CF_3), 126.91 (CF_3)	2.159 (2.917), 2.029 (2.831)
oCF_3HPU	*c* (Type I)	132.93 (CF_3), −142.42 (H)	2.074 (2.849), 2.272 (2.948)
*o*ClPU	*b* (Type I)	(mol 1) −43.68 (Cl), −43.68 (Cl); (mol 2) 47.88 (Cl), 47.88 (Cl)	2.056 (2.863), 2.056 (2.863)
*o*ClHPU	*a* (Type II)	43.94 (Cl), −36.08 (H)	2.081 (2.884), 2.065 (2.871)
*o*CyPU	none (Type III)	−175.44 (Cy), 168.42 (Cy)	N/A
*o*CyHPU	none (Type III)	−178.60 (Cy), 178.99 (H)	N/A
*o*EPU	none (Type III)	−166.98 (E), −176.08 (E)	N/A
*o*IHPU	*b* (Type I)	−124.61 (I), −130.62 (H)	2.188 (2.925), 2.094 (2.866)
α-*o*MoPU	*c* (Type I)	−138.12 (Mo), −138.12 (Mo)	2.243 (2.996), 2.243 (2.996)
β-*o*MoPU	*c* (Type II)	156.55 (Mo), 156.55 (Mo)	2.331 (3.144), 2.331 (3.144)
α-*o*NPU	*b* (Type I)	−42.07 (N), −37.75 (N)	2.156 (2.915), 2.038 (2.844)
β-*o*NPU	none (Type III)	(mol 1) 174.65 (N), 176.95 (N); (mol 2) −153.32 (N), 167.86 (N)	N/A
α-*o*NHPU	*a* (Type I)	138.08 (N), −136.79 (H)	2.240 (2.949), 2.118 (2.850)
β-*o*NHPU	*a* (Type I)	−51.64 (N), −55.57 (H)	2.116 (2.866), 2.133 (2.912)

was selected. In all cases, the *anti*−*anti* conformation was found to be lowest in energy, and all energy optimizations were considered relative to these minima.

RESULTS AND DISCUSSION

The compounds in this study are named as *o*XPU and *o*XHPU, depending on whether both or only one aromatic ring bears an ortho-substituent. X represents the substituent with A = amino, Br = bromo, CF_3 = trifluoromethyl, Cl = chloro, Cy = cyano, E = methylester, Mo = methoxy, and N = nitro. The X-ray data for all new crystal forms obtained from our polymorph screening of *o*NPU, *o*NHPU, *o*CF_3PU, *o*CF_3HPU, *o*ClPU, *o*ClHPU, *o*CyPU, and *o*CyHPU appear in Table 1. The previously reported structures include two polymorphs of oMoPU (refcode: SILTUC, SILTUC01)[25] and single structures of *o*BrPU (refcode: AQASIV),[34] *o*EPU (refcode: XULHUJ),[35] *o*IHPU (refcode: AVADIM),[36] *o*AHPU (refcode: LOYDAG),[37] and *α*-*o*NPU (refcode: VIRVAV).[38] An entry for *o*ClPU (refcode: QQQAGD)[39] lacked 3D coordinates and has a different unit cell than the one obtained in our work. The X-ray data for *o*MoPU, *o*BrPU, *o*EPU, *o*IHPU, *o*AHPU and *α*-*o*NPU appear in Table S1.

Analysis of the 16 *o*XPU and *o*XHPU structures (Tables 1 and S1) reveals a variety of packing motifs, with only one pair that is isostructural. In an effort to discuss the similarities and differences across all structures, we sort them into three general categories based on their hydrogen bonding topologies (Figure 1). A majority of structures exhibit the classic one-dimensional $[C(4)R_2^1(6)]$ bonding motif between urea groups. This motif can form between molecules related by translation (Type I) or between molecules that twist about the chain axis (Type II). In some systems, hydrogen bonding between the ortho-substituent and the urea group (Type III) is observed. For the new compounds examined here, the crystallization into either a needle or prismatic morphology proved to be a good indicator for the presence or absence of the $[C(4)R_2^1(6)]$ motif, respectively.

Structure Type I. Type I, the first and largest group, consists of 10 structures. This includes (a) *α*-*o*NHPU, (b) *β*-*o*NHPU, (c) *o*CF_3PU, (d) *o*ClPU, (e) *α*-*o*NPU (VIRVAV), (f) *o*AHPU (LOYDAG), (g) *α*-*o*MoPU (SILTUC), (h) *o*BrPU (AQASIV), and (i) *o*CF_3HPU. In the classic $[C(4)R_2^1(6)]$ bonding motif, the N−H···O distances range from 1.94 to 2.27 Å; N···O distances from 2.77 to 2.99 Å (Table 2). Molecules within the chain are related by translation about a short axis (4.56−4.75 Å); however, the short axis corresponds to the *a*-, *b*-, or *c*-crystallographic axis in different structures. Type I structures differ from one another in two key respects: the relative orientation of urea chains (e.g., parallel vs antiparallel) and/or the symmetry relationships between chains.

Packing diagrams for the Type I structures appear in Figure 2. All are viewed down the 1D hydrogen bonding axis.

DOI: 10.1021/acs.cgd.7b00757
Cryst. Growth Des. XXXX, XXX, XXX−XXX

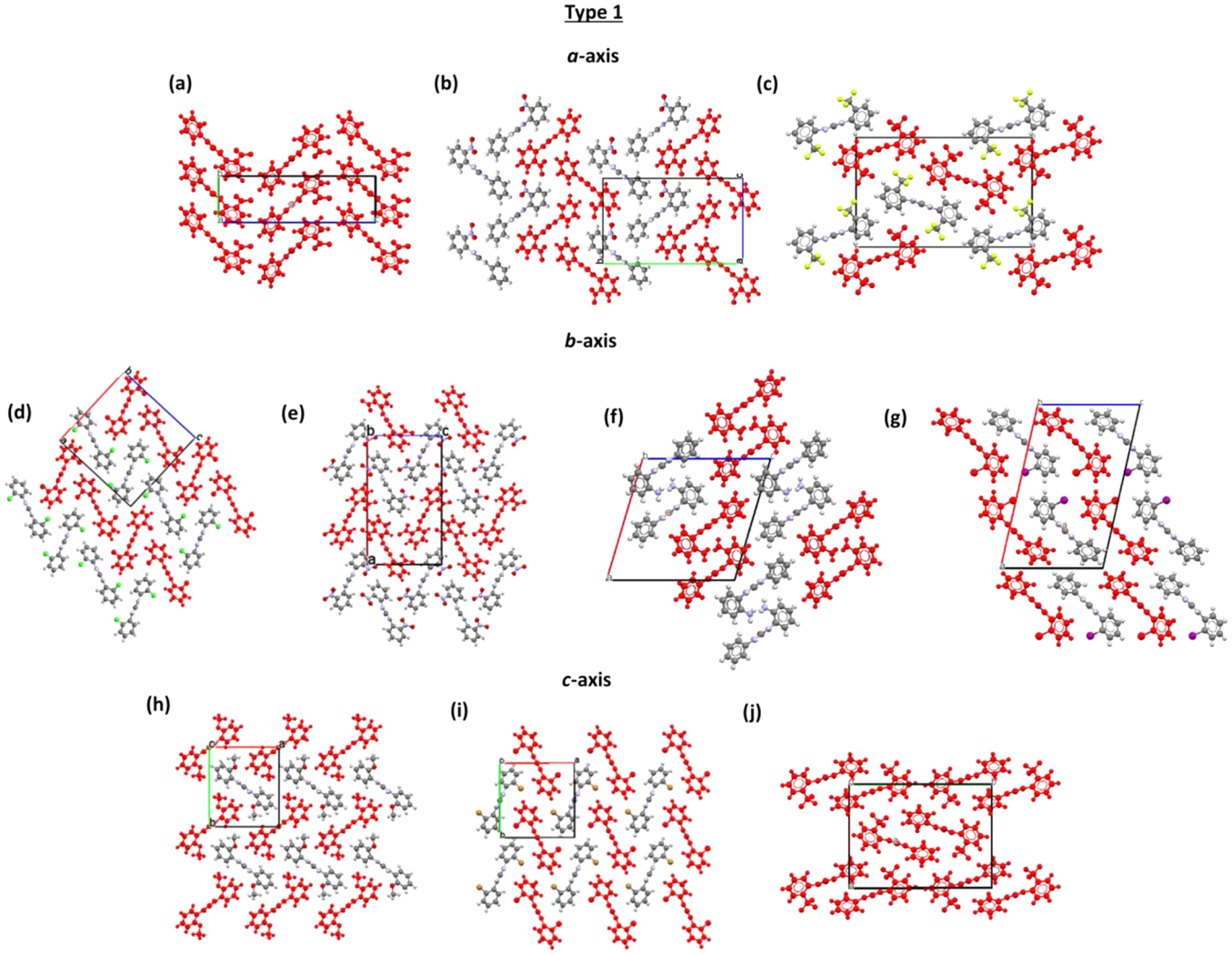

Figure 2. Type I *o*PU structures. All packing diagrams are viewed down the short hydrogen bonding axis. Molecules are color coded to reflect the absolute orientation of the chain. Red chains are oriented with the carbonyl group up; chains colored by atom type are oriented with the amino end up. View down *a*-axis: (a) *α*-*o*NHPU, (b) *β*-*o*NHPU, and (c) *o*CF_3PU. View down *b*-axis: (d) *o*ClPU, (e) *α*-*o*NPU, (f) *o*AHPU, and (g) *o*IHPU. View down *c*-axis: (h) *α*-*o*MoPU, (i) *o*BrPU, and (j) *o*CF_3HPU.

Molecules are colored to indicate the absolute direction of the urea chain. Red chains are oriented with the carbonyl group up; chains colored by atom type are oriented with the amino end up. In eight of the *o*PU structures, urea chains adopt an antiparallel alignment. However, in two cases, *α*-*o*NHPU and *o*CF_3HPU, urea chains align in parallel. A survey of all 1,3-diphenylurea structures in the CSD shows this packing arrangement is fairly rare, occurring in only ∼4 other entries.[40] The orientation of molecules in these two structures differ significantly, with the molecules mutually aligned (related by translation) along one axis in the former and dimer units in the latter.

None of the eight structures with antiparallel urea chains are isostructural, though the differences between them are more subtle and arise from differences in the symmetry elements with respect to the chain direction (Figure S1). In cases where the urea chain parallels the *a*-axis, glide planes and 2-fold rotation axes run parallel to the chain. When the urea chain parallels the *b*-axis, the urea chains intersect glide planes. The structures with *c*-axis urea chains have perpendicular 2-fold axes and/or glide planes that parallel the urea axis. Notably, the three Type I (*c*-axis) structures (*β*-*o*MoPU, *o*BrPU, and *o*CF_3HPU) do not have inversion symmetry.

Structure Type II. The two members of class Type II, (k) *β*-*o*OMePU (SILTUC01) and (l) *o*ClHPU, also form 1D $[C(4)R_2^1(6)]$ urea chains; however, in both cases, the molecules rotate about the urea axis (Figures 3 and S2). The unusual $P4_2/n$ space group of *β*-*o*OMePU (SILTUC01) results in a 90° rotation of adjacent molecules within the urea chain. Molecules in the urea chain of *o*ClHPU twist along a 2_1 screw axis. The repeat distance along the twisted chain (9.18−9.83 Å) is roughly double the repeat length observed in Type I *o*PUs, such that the urea hydrogen bonding distances in Type I and Type II are equivalent. In both Type II structures, the adjacent urea chains are antiparallel for net centrosymmetry.

Structure Type III. The four structures shown in Figure 4, (m) *o*EPU, (n) *o*CyHPU, (o) *β*-*o*NPU, and (p) *o*CyPU, are classified as Type III. They share two features in common. First, their torsion angles about the C(O)−N−C−C bonds are significantly more planar than the other *o*PUs (see Table 2). The more planar conformations allow for weak hydrogen C−H···O interactions between the *ortho* hydrogen atoms and the urea carbonyl group. The second common feature is the

DOI: 10.1021/acs.cgd.7b00757
Cryst. Growth Des. XXXX, XXX, XXX−XXX

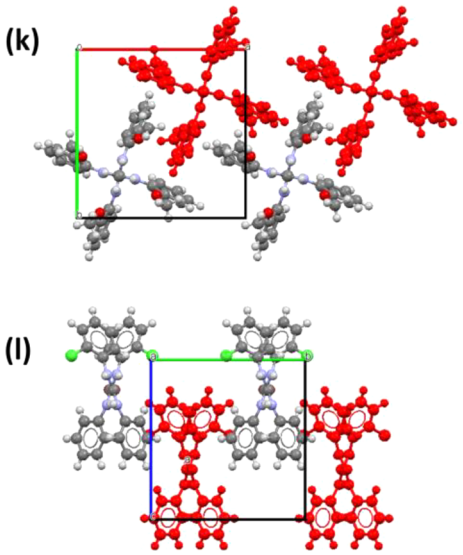

Figure 3. Type II *o*PU structures. Red chains are oriented with the carbonyl group up; chains colored by atom type are oriented with the amino end up. (k) *β*-*o*MoPU is viewed down the *c*-axis. (l) *o*ClHPU is viewed down the *a*-axis.

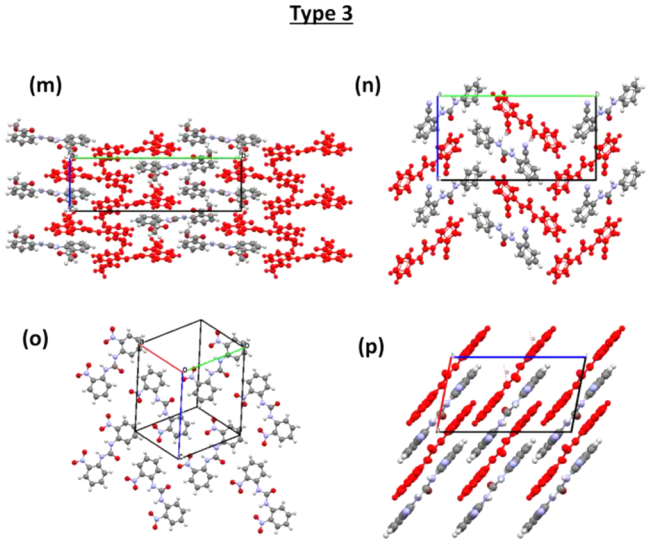

Figure 4. Type III *o*PU structures include (m) *o*EPU, (n) *o*CyHPU, (o) *β*-*o*NPU, and (p) *o*CyPU. The carbonyl group of the urea is oriented up in molecules colored in red and down in molecules colored by atom type.

absence of a 1D hydrogen-bonded urea chain. Beyond that, the four structures differ significantly. Two exhibit intramolecular bonding between the ortho-substituent and the urea (scheme (d) in Figure 1), one exhibits intermolecular hydrogen bonding between ortho-substituents and urea (scheme (c) in Figure 1), and the fourth oddly exhibits no strong hydrogen bonding at all.

Intramolecular S(6) bonds between the ortho-substituent and urea are seen in (m) *o*EPU and (o) *β*-*o*NPU. In *o*EPU, O···H−N bonds are 1.918 and 1.961 Å (O···N, 2.659 and 2.677 Å). *β*-*o*NPU has two molecules in the asymmetric unit, and the O···H−N contacts range between 1.835 and 2.015 Å (O···N, 2.603−2.676 Å). Neither structure exhibits strong intermolecular hydrogen bonding, either between urea groups or between urea and ortho-substituents. *β*-*o*NPU has some additional features of interest. Three of the four nitro groups are twisted by ∼10° out of the plane of the aromatic ring, the fourth is twisted out of the plane by ∼24°. This allows molecules to assemble into nearly planar polar sheets in the (110) plane, indicating that *π*−*π* interactions play an important role in the overall lattice energy.

With nitrile substituents, the structures of *o*CyHPU (n) and *o*CyPU (p) were unlike any others in this study. *o*CyHPU adopts a unique cyclic $R_2^2(16)$ dimer motif formed from two pairs of hydrogen bonds between the ortho-substituent of one molecule and the urea NH group of the other. Both bonds within the dimer have an N···H−N distance of 2.119 Å (N···N, 2.993 Å). The nearly planar dimer pairs form close packed *π*−*π* assemblies in the (101) plane. The most unusual structure across the entire series of compounds investigated was *o*CyPU. Despite its multiple hydrogen bond donors and acceptors, none are fulfilled. The *π*−*π* interactions appear to be dominant, with face-to-face stacks aligned along the [101] axis. The ability for both nitro and nitrile substituents to disrupt the formation of 1D urea chains is not entirely surprising, as it was also seen in polymorphism studies of the meta-substituted diphenylurea analogues.[14,16,41] However, in these previous studies the hydrogen bond donors and acceptors were satisfied either partially or fully in all of the polymorphs identified. *o*CyPU is truly unusual in that it does not.

Polymorphism. A recent review by Cruz-Cabeza and Bernstein[42] reported that 36% of all polymorphic molecules exhibit conformational polymorphism. In our previous analyses of meta-substituted diphenylureas, we were able to identify conformational polymorphs in some systems[16,17,43] but not others.[15] We assumed this would also be the case for *o*PUs. Orthorhombic and monoclinic polymorphs of *o*MoPU were previously reported by Etter et al.[44] Both *α*- and *β*-forms exhibit 1D urea chains, though molecules can either be related by translation (*α*, Type I) or twisted (*β*, Type II). A basic solvent screen was applied to the new *o*PUs in this study. PXRD and thermal analysis identified three polymorphic systems: *o*NPU, *o*NHPU, and *o*CyHPU. This does not preclude the possibility that other polymorphic systems might be found at some later date through a more exhaustive survey of crystallization conditions.

The structure of *o*NPU, which we now refer to as *α*, had been previously reported (refcode: VIRVAV).[38] In our polymorph screen, we obtained this yellow form from multiple growth solutions, as well as colorless crystals of *β*-*o*NPU from recrystallization in benzene. Not only do *α*- and *β*-*o*NPU have different hydrogen boding motifs (Type I and III), they have very different amide torsion angles (see Table 2) and torsions between the nitro groups and the plane of the aromatic ring. In *α*, the nitro out-of-plane torsion angles are 15.8−17.8° and in *β* they range from 3.6 to 23.8°. The *α*- and *β*-*o*NHPU forms were identified by the presence of two endotherms in the DSC of the initially precipitated material, indicating these crystallize concomitantly. Recrystallization from assorted solvents yielded yellow *α*-needles from acetone and colorless *β*-needles from ethanol. Though both *α* and *β* adopt Type I motifs, the former is a polar phase and the latter centrosymmetric. Differences also exist in both the amide and nitro torsion angles.

Evidence suggested that *o*CyHPU is also polymorphic (Figures 5 and S3). Clear prisms obtained from ethanol melt at approximately 181 °C. The yellow melt rapidly solidifies to a polycrystalline material, which begins to melt at 195 °C. Comparison of the *o*CyHPU PXRD patterns of the colorless

DOI: 10.1021/acs.cgd.7b00757
Cryst. Growth Des. XXXX, XXX, XXX−XXX

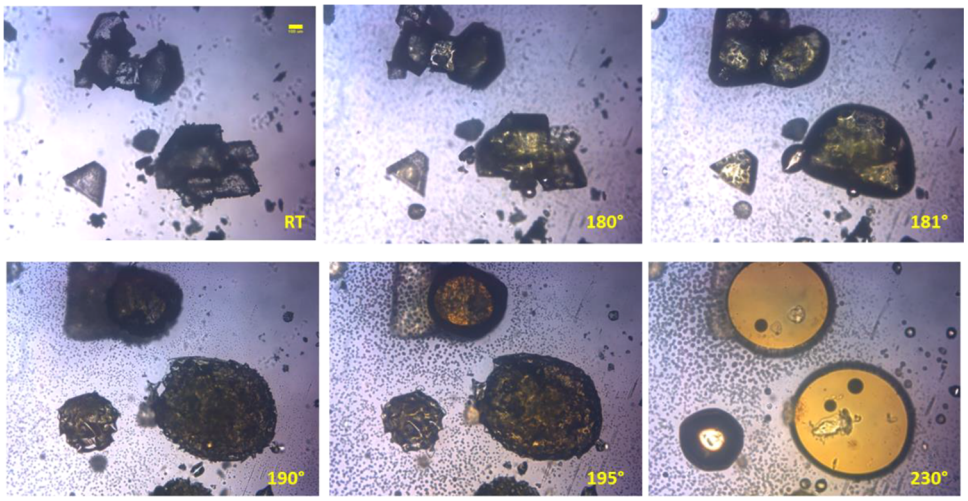

Figure 5. HSM of *o*CyHPU prisms showing a phase transition to a second, unidentified polymorph from melt recrystallization.

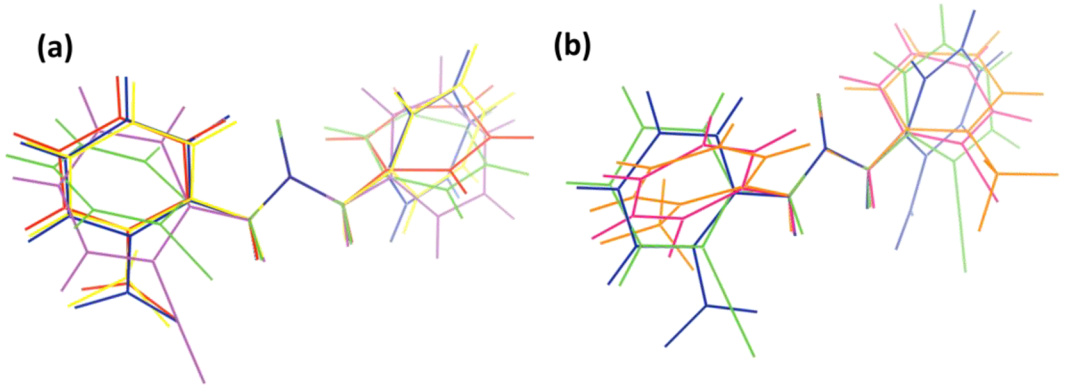

Figure 6. Overlays of *o*PU molecular conformations obtained from single crystal structures. Monosubstitued systems are shown in (a): *o*CyHPU (purple), *o*ClHPU (green), *o*CF_3HPU (yellow), *α*-*o*NHPU (red), and *β*-*o*NHPU (blue). Disubstitued systems are shown in (b): *β*-*o*NPU (blue), *o*CF_3PU (orange), *o*ClPU (magenta), and *o*CyPU (green).

prism and the melt-recrystallized phase show they are clearly different, though we have so far been unable to obtain high-quality single crystals of the latter.

Molecular Conformation. Rotation about the amide bond allows PUs to adopt multiple conformations. For disubstituted compounds, these can broadly be described as *anti*−*anti*, *anti*−*syn*, and *syn*−*syn* based on the relative orientation of the ortho-substituents with respect to the carbonyl group. Monosubstituted compounds can similarly adopt *anti* or *syn* conformations. All the *o*PU structures were found to adopt *anti*−*anti* or *anti* conformations, though a range of C(O)−N−C−C torsion angles is seen. Many have torsions >100°, twisting the phenyl rings nearly perpendicular to the urea groups. Figure 6 overlays the conformations of *o*XHPU and *o*XPUs observed in single crystals (for specific angles see Table 2).

The crystal structures of PUs bearing meta-substituents show a much greater range of torsion angles about the urea bond. The fact that all *o*PU structures adopted *anti*−*anti*/*anti* conformations suggested the barrier to free rotation was higher than in the corresponding meta-substituted PUs. To test this hypothesis, the conformations of *o*ClPU, *o*ClHPU, and *m*ClPU monomers with fixed torsion angles were subjected to geometric optimizations in Gaussian09. The aromatic rings were initially fixed with C(O)−N−C−C torsion angles of 180/−180° or an *anti*−*syn* conformation. The substituent-bearing ring was then rotated sequentially in 10° increments toward the *anti*−*anti* conformation. The second aromatic ring in the disubstituted systems was then rotated to achieve a planar *syn*−*anti* conformation (identical to the original *anti*−*syn*).

The planar *anti*−*anti*/*anti* conformations of each compound were found to be lowest in energy, though there are clear differences in the rotational barrier of the three. All optimized energies plotted in Figure 7 are relative to the *anti*−*anti*/*anti* conformation. For *o*ClPU, the planar *anti*−*syn* conformation was highest in energy. Rotation of the ortho-chlorophenyl ring in *o*ClHPU resulted in a similar trend, yielding an approximate rotational barrier of ∼15 kcal/mol for each ring. The rotational barrier in *m*ClPU, initially reported in a previous work,[15] was recalculated here with an improved basis set. The rotational barrier in *m*ClPU was only one-third that of *o*ClPU and *o*ClHPU, or ∼5 kcal/mol. Figure 7 also illustrates that while the *anti*−*anti* and *anti*−*syn* conformations of *m*ClPU are energetically similar, this is not the case with *o*PUs, whose *anti*−*syn* conformations are the highest in energy. The significantly larger energy difference between *syn* and *anti* *o*PU conformations affects their relative population in solution and helps to explain why only *anti*−*anti*/*anti* molecular conformations were observed in structural studies. Given the wide range of low energy conformations that is covered by our definition of *anti* geometries, it is not clear to what extent, if any, restricted rotations limit the ability of *o*PUs to crystallize as conformational polymorphs.

DOI: 10.1021/acs.cgd.7b00757
Cryst. Growth Des. XXXX, XXX, XXX−XXX

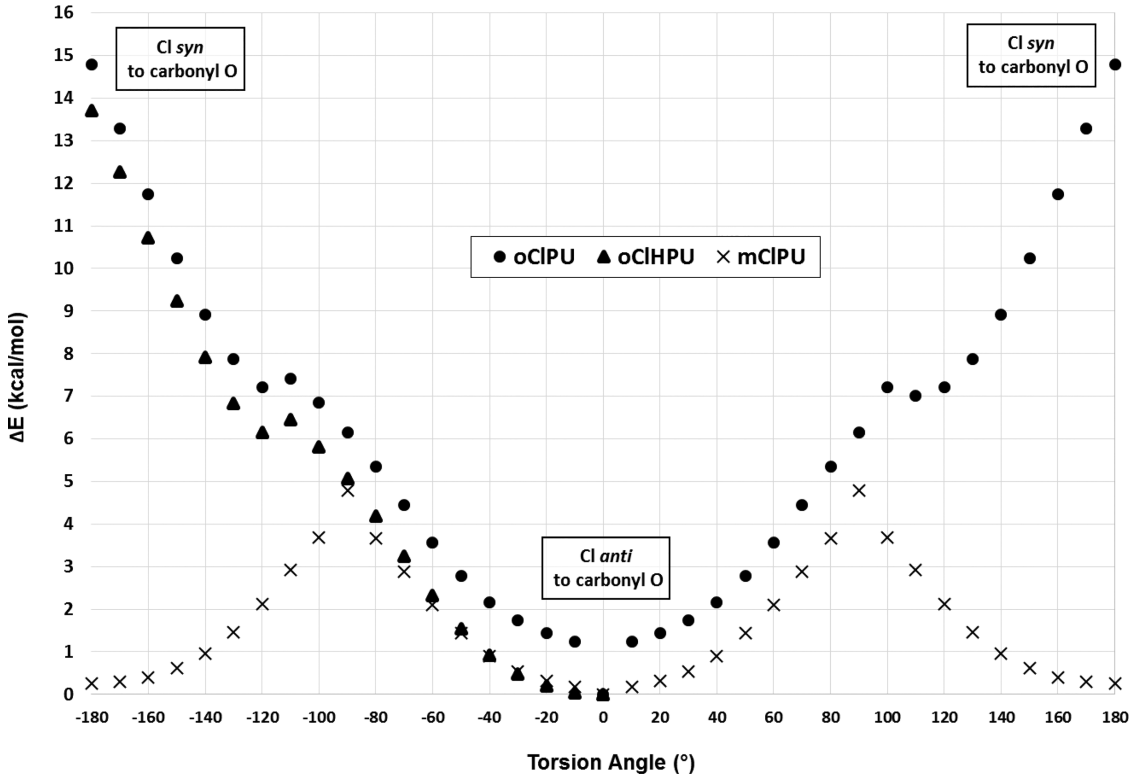

Figure 7. Rotational barrier about the amide bond of *o*ClPU, *o*ClHPU, and *m*ClPU. *Syn* conformations were the highest in energy in *o*ClPU and *o*ClHPU, which may explain why they are typically not observed in *o*PUs. In *o*ClPU and *o*ClHPU, *syn* conformations were the highest in energy, which may explain why they are typically not observed in *o*PU systems.

CONCLUSIONS

The 16 total (nine new) *o*PU structures analyzed in this study exhibit an interesting diversity of hydrogen bonding motifs (urea chains, intramolecular and dimeric motifs), as well as packing arrangements (polar, nonpolar, and symmetry relations). All of the molecular conformations observed were *anti*−*anti*/*anti*, which is consistent with the calculated barrier for rotation about the amide bond. Four of the 13 systems analyzed were shown to exhibit polymorphism. Though 13 systems are a relatively small data set, and additional polymorphs may be found with an expanded screen, it seems that when substituents can compete with urea as a hydrogen bond acceptor, *o*PUs may be generally more likely to crystallize in multiple forms. It is less clear whether diphenylurea structures with H-bond donors in ortho-positions are likely to exhibit polymorphism since so few have been reported. Any intramolecular hydrogen bonds would require a *syn* conformation, which seems less likely in view of their higher conformational energies. Intermolecular H-bonding between substituent H-bond donors and urea acceptors is still possible with an *anti* conformation, as is the case for *o*APU (LOYDAG).

Restricted amide bond rotation has been suggested to confer specific advantages in other fields such as in drug binding[45,46] and/or stereochemical recognition (atropisomerism).[47−49] Notably, a relatively high proportion of *o*PU structures are noncentrosymmetric. This observation hints that restricted conformations, which lock the PUs into a chiral conformation, may provide a helpful bias toward crystallization in acentric space groups.

ASSOCIATED CONTENT

Supporting Information

The Supporting Information is available free of charge on the ACS Publications website at DOI: 10.1021/acs.cgd.7b00757.

Additional PXRD data for *o*CyHPU (PDF)

Accession Codes

CCDC 1504100−1504106 and 1504132−1504133 contain the supplementary crystallographic data for this paper. These data can be obtained free of charge via www.ccdc.cam.ac.uk/data_request/cif, or by emailing data_request@ccdc.cam.ac.uk, or by contacting The Cambridge Crystallographic Data Centre, 12 Union Road, Cambridge CB2 1EZ, UK; fax: +44 1223 336033.

AUTHOR INFORMATION

Corresponding Author

*E-mail: jas2@georgetown.edu.

ORCID

Jennifer A. Swift: 0000-0002-8011-781X

Notes

The authors declare no competing financial interest.

ACKNOWLEDGMENTS

The authors are grateful for financial support provided by the National Science Foundation under awards CHE-1156788 (REU), CHE-0959546 (MRI), and CHE-1337975 (MRI). M.A.S. thanks the ARCS Foundation for a predoctoral fellowship. We additionally thank Jeffery Bertke for assistance with the refinement of *o*CF_3HPU and Maxime Siegler (Johns

DOI: 10.1021/acs.cgd.7b00757
Cryst. Growth Des. XXXX, XXX, XXX−XXX

Hopkins University) for his help collecting diffraction data for three *o*PUs and assistance in refining *o*ClHPU.

REFERENCES

(1) Voogd, T. E.; Vansterkenburg, E. L.; Wilting, J.; Janssen, L. H. *Pharmacol. Rev.* **1993**, *45*, 177.
(2) Li, G.-B.; Ma, S.; Yang, L.-L.; Ji, S.; Fang, Z.; Zhang, G.; Wang, L.-J.; Zhong, J.-M.; Xiong, Y.; Wang, J.-H.; Huang, S.-Z.; Li, L.-L.; Xiang, R.; Niu, D.; Chen, Y.-C.; Yang, S.-Y. *J. Med. Chem.* **2016**, *59*, 8293.
(3) Li, H.-Q.; Lv, P.-C.; Yan, T.; Zhu, H.-L. *Anti-Cancer Agents Med. Chem.* **2009**, *9*, 471.
(4) Jin, F.; Gao, D.; Zhang, C.; Liu, F.; Chu, B.; Chen, Y.; Chen, Y. Z.; Tan, C.; Jiang, Y. *Bioorg. Med. Chem.* **2013**, *21*, 824.
(5) Gatidou, G.; Stasinakis, A. S.; Iatrou, E. I. *Chemosphere* **2015**, *119*, S69.
(6) Tixier, C.; Bogaerts, P.; Sancelme, M.; Bonnemoy, F.; Twagilimana, L.; Cuer, A.; Bohatier, J.; Veschambre, H. *Pest Manage. Sci.* **2000**, *56*, 455.
(7) Sheets, T. J. *Weeds* **1958**, *6*, 413.
(8) Schebb, N. H.; Inceoglu, B.; Ahn, K. C.; Morisseau, C.; Gee, S. J.; Hammock, B. D. *Environ. Sci. Technol.* **2011**, *45*, 3109.
(9) Halden, R. U. *Environ. Sci. Technol.* **2014**, *48*, 3603.
(10) Halden, R. U.; Paull, D. H. *Environ. Sci. Technol.* **2005**, *39*, 1420.
(11) Shimizu, L. S.; Salpage, S. R.; Korous, A. A. *Acc. Chem. Res.* **2014**, *47*, 2116.
(12) Steed, J. W. *Chem. Commun.* **2011**, *47*, 1379.
(13) Cho, Y. L.; Rudkevich, D. M.; Rebek, J. *J. Am. Chem. Soc.* **2000**, *122*, 9868.
(14) Hiremath, R.; Basile, J. A.; Varney, S. W.; Swift, J. A. *J. Am. Chem. Soc.* **2005**, *127*, 18321.
(15) Capacci-Daniel, C.; Dehghan, S.; Wurster, V. M.; Basile, J. A.; Hiremath, R.; Sarjeant, A. A.; Swift, J. A. *CrystEngComm* **2008**, *10*, 1875.
(16) Capacci-Daniel, C. A.; Mohammadi, C.; Urbelis, J. H.; Heyrana, K.; Khatri, N. M.; Solomos, M. A.; Swift, J. A. *Cryst. Growth Des.* **2015**, *15*, 2373.
(17) Capacci-Daniel, C. A.; Bertke, J. A.; Dehghan, S.; Hiremath-Darji, R.; Swift, J. A. *Acta Crystallogr., Sect. C: Struct. Chem.* **2016**, *C72*, 692.
(18) Reddy, L. S.; Basavoju, S.; Vangala, V. R.; Nangia, A. *Cryst. Growth Des.* **2006**, *6*, 161.
(19) Reddy, L. S.; Chandran, S. K.; George, S.; Babu, N. J.; Nangia, A. *Cryst. Growth Des.* **2007**, *7*, 2675.
(20) Huang, K.-S.; Britton, D.; Etter, M. C.; Byrn, S. R. *J. Mater. Chem.* **1995**, *5*, 379.
(21) George, S.; Nangia, A.; Lam, C.-K.; Mak, T. C. W.; Nicoud, J.-F. *Chem. Commun.* **2004**, 1202.
(22) Velikova, V.; Angelova, O.; Kossev, K. *Acta Crystallogr., Sect. C: Cryst. Struct. Commun.* **1997**, *C53*, 1273.
(23) Kudo, M.; Hanashima, T.; Muranaka, A.; Sato, H.; Uchiyama, M.; Azumaya, I.; Hirano, T.; Kagechika, H.; Tanatani, A. J. *J. Org. Chem.* **2009**, *74*, 8154.
(24) Etter, M. C.; Panunto, T. W. *J. Am. Chem. Soc.* **1988**, *110*, 5896.
(25) Etter, M. C.; Urbanczyk-Lipkowska, Z.; Zia-Ebrahimi, M.; Panunto, T. W. *J. Am. Chem. Soc.* **1990**, *112*, 8415.
(26) Solomos, M. A.; Mohammadi, C.; Urbelis, J. H.; Koch, E. S.; Osborne, R.; Usala, C. C.; Swift, J. A. *Cryst. Growth Des.* **2015**, *15*, 5068.
(27) Perveen, S.; Abdul Hai, S. M.; Khan, R. A.; Khan, K. M.; Afza, N.; Sarfaraz, T. B. *Synth. Commun.* **2005**, *35*, 1663.
(28) Naegeli, C.; Tyabji, A.; Conrad, L. *Helv. Chim. Acta* **1938**, *21*, 1127.
(29) Dyer, E.; McCormick, K. L. *J. Am. Chem. Soc.* **1946**, *68*, 986.
(30) Adler, T.; Bonjoch, J.; Clayden, J.; Font-Bardía, M.; Pickworth, M.; Solans, X.; Solé, D.; Vallverdú, L. *Org. Biomol. Chem.* **2005**, *3*, 3173.
(31) Borsche, W.; Sander, W. *Ber. Dtsch. Chem. Ges.* **1914**, *47*, 2815.
(32) Sheldrick, G. M. *Program for Empirical Absorption Correction of Area Detector Data*; University of Gottingen: Germany, 1996.
(33) Sheldrick, G. M. *Acta Crystallogr., Sect. A: Found. Crystallogr.* **2008**, *A64*, 112.
(34) Huth, S. L.; Threlfall, T. L.; Hursthouse, M. B. *Crystal Structure Report Archive*; University of Southampton, **2008**. DOI: 10.5258/ecrystals/689.
(35) Yassine, H.; Khouili, M.; El Ammari, L.; Saadi, M.; Ketatni, E. M. *Acta Crystallographica Section E* **2015**, *71*, o297.
(36) Koshti, V. S.; Thorat, S. H.; Gote, R. P.; Chikkali, S. H.; Gonnade, R. G. *CrystEngComm* **2016**, *18*, 7078.
(37) Mague, J. T.; Mohamed, S. K.; Akkurt, M.; Omran, O. A.; Albayati, M. R. *Acta Cryst. E* **2015**, *E71*, o88.
(38) Kirby, I. L.; Pitak, M. B.; Wenzel, M.; Wilson, C.; Sparkes, H. A.; Coles, S. J.; Gale, P. A. *CrystEngComm* **2013**, *15*, 9003.
(39) Deshapande, S. V.; Meredith, C. C.; Pasternak, R. A. *Acta Crystallogr., Sect. B: Struct. Crystallogr. Cryst. Chem.* **1968**, *B24*, 1396.
(40) PUs with parallel chains include (LENXOT), (SILTOW01), (TIVQEV), and (AQATIW02).
(41) Rafilovich, M.; Bernstein, J.; Harris, R. K.; Apperley, D. C.; Karamertzanis, P. G.; Price, S. L. *Cryst. Growth Des.* **2005**, *5*, 2197.
(42) Cruz-Cabeza, A. J.; Bernstein, J. *Chem. Rev.* **2014**, *114*, 2170.
(43) Capacci-Daniel, C.; Gaskell, K. J.; Swift, J. A. *Cryst. Growth Des.* **2009**, *10*, 952.
(44) Etter, M. C.; Urbanczyk-Lipkowska, Z.; Zia-Ebrahimi, M.; Panunto, T. W. *J. Am. Chem. Soc.* **1990**, *112*, 8415.
(45) Qiao, J. X.; Wang, T. C.; Ruel, R.; Thibeault, C.; L'Heureux, A.; Schumacher, W. A.; Spronk, S. A.; Hiebert, S.; Bouthillier, G.; Lloyd, J.; Pi, Z.; Schnur, D. M.; Abell, L. M.; Hua, J.; Price, L. A.; Liu, E.; Wu, Q.; Steinbacher, T. E.; Bostwick, J. S.; Chang, M.; Zheng, J.; Gao, Q.; Ma, B.; McDonnell, P. A.; Huang, C. S.; Rehfuss, R.; Wexler, R. R.; Lam, P. Y. S. *J. Med. Chem.* **2013**, *56*, 9275.
(46) Chao, H.; Turdi, H.; Herpin, T. F.; Roberge, J. Y.; Liu, Y.; Schnur, D. M.; Poss, M. A.; Rehfuss, R.; Hua, J.; Wu, Q.; Price, L. A.; Abell, L. M.; Schumacher, W. A.; Bostwick, J. S.; Steinbacher, T. E.; Stewart, A. B.; Ogletree, M. L.; Huang, C. S.; Chang, M.; Cacace, A. M.; Arcuri, M. J.; Celani, D.; Wexler, R. R.; Lawrence, R. M. *J. Med. Chem.* **2013**, *56*, 1704.
(47) Clayden, J.; Turner, H.; Helliwell, M.; Moir, E. J. *J. Org. Chem.* **2008**, *73*, 4415.
(48) Kumarasamy, E.; Raghunathan, R.; Sibi, M. P.; Sivaguru, J. *Chem. Rev.* **2015**, *115*, 11239.
(49) Clayden, J.; Lemiegre, L.; Pickworth, M.; Jones, L. *Org. Biomol. Chem.* **2008**, *6*, 2908.

DOI: 10.1021/acs.cgd.7b00757
Cryst. Growth Des. XXXX, XXX, XXX−XXX